22. Artini, M. *et al.* Elevated serum levels of 90K/MAC-2 BP predict unresponsiveness to alpha-interferon therapy in chronic HCV hepatitis patients. *J. Hepatol.* **25**, 212–217 (1996).
23. Cheung, K. J. *et al.* The HCV serum proteome: a search for fibrosis protein markers. *J. Viral. Hepat.* **16**, 418–429 (2009).
24. Kuno, A. *et al.* Focused differential glycan analysis with the platform antibody-assisted lectin profiling for glycan-related biomarker verification. *Mol. Cell. Proteomics* **8**, 99–108 (2008).
25. Kuno, A. *et al.* Evanescent-field fluorescence-assisted lectin microarray: a new strategy for glycan profiling. *Nat. Met.* **2**, 851–856 (2005).
26. Vallet-Pichard, A. *et al.* FIB-4: an inexpensive and accurate marker of fibrosis in HCV infection. Comparison with liver biopsy and fibrotest. *Hepatology* **46**, 32–36 (2007).
27. Ito, K. *et al.* LecT-Hepa, a glyco-marker derived from multiple lectins, as a predictor of liver fibrosis in chronic hepatitis C patients. *Hepatology* **56**, 1448–1456 (2012).
28. Bruno, S. *et al.* Sustained virological response to interferon-α is associated with improved outcome in HCV-related cirrhosis: A retrospective study. *Hepatology* **45**, 579–587 (2007).
29. Cardoso, A.-C. *et al.* Impact of peginterferon and ribavirin therapy on hepatocellular carcinoma: Incidence and survival in hepatitis C patients with advanced fibrosis. *J. Hepatol.* **52**, 652–657 (2010).
30. Morgan, T. R. *et al.* Outcome of sustained virological responders with histologically advanced chronic hepatitis C. *Hepatology* **52**, 833–844 (2010).
31. Lupberger, J. *et al.* EGFR and EphA2 are host factors for hepatitis C virus entry and possible targets for antiviral therapy. *Nat. Med.* **17**, 589–595 (2011).
32. Iwasaki, Y. *et al.* Risk factors for hepatocellular carcinoma in hepatitis C patients with sustained virologic response to interferon therapy. *Liver Int.* **24**, 603–610 (2004).
33. Ikeda, K. *et al.* Anticarcinogenic impact of interferon on patients with chronic hepatitis C: A large-scale long-term study in a single center. *Intervirology* **49**, 82–90 (2006).
34. Kurosaki, M. *et al.* Data mining model using simple and readily available factors could identify patients at high risk for hepatocellular carcinoma in chronic hepatitis C. *J. Hepatol.* **56**, 602–608 (2012).
35. Schuppan, D. & Pinzani, M. Anti-fibrotic therapy: lost in translation? *J. Hepatolol.* **56**, S66–74 (2012).
36. Rizzo, L. *et al.* Comparison of transient elastography and acoustic radiation force impulse for non-invasive staging of liver fibrosis in patients with chronic hepatitis C. *Am. J. Gastroenterol.* **106**, 2112-2120 (2011).
37. Ferraioli, G. *et al.* Performance of real-time sitrain elastography, transient elastgraphy, and aspartate-to-platelet ration index in the assessment of fibrosis in chronic hepatitis C. *AJR Am. J. Roentgenol.* **199**, 19–25 (2012).
38. Poynard, T. *et al.* Standardization of ROC curve areas for diagnostic evaluation of liver fibrosis markers based on prevalences of fibrosis stages. *Clin. Chem.* **53**, 1615–1622 (2007).
39. Nishimura, S. Toward automated glycan analysis. *Adv. Carbohydr. Chem. Biochem.* **65**, 219–271 (2011).

Acknowledgments

This work was supported in part by a grant from New Energy and Industrial Technology Development Organization of Japan. We thank H. Ozaki, H. Shimazaki, S. Unno, K. Saito, M. Sogabe, Y. Kubo, J. Murakami, S. Shirakawa, T. Fukuda (AIST), and H. Naganuma (NCU) for technical assistance. We also thank A. Togayachi, T. Sato, H. Kaji, J. Hirabayashi, H. Tateno, A. Takahashi (AIST) and C. Tsuruno, S. Nagai and Y. Takahama (Sysmex Co.) for critical discussion.

Author contributions:

A.K. conceived and designed the study, performed most of the biochemical experiments, analyzed data and wrote the paper with comments from Y.T., M.M. and H.N.; Y.I. conceived and designed the study, performed the sample pre-treatment for the assay, and analyzed data; Y.T., K.I., M.M., and S.H collected clinical samples, designed the validation study, and analyzed data; A.M. and S.S. performed the biochemical experiments including lectin microarray analysis and analyzed data; M.S. and M.K. performed staging of biopsy specimens by histological activity index (HAI); H.N. conceived and designed the study, and supervised all aspects of the work; and all authors discussed the results and implications, and commented on the paper.

Additional information

Supplementary information accompanies this paper at http://www.nature.com/scientificreports

Competing financial interests: The authors declare no competing financial interests.

License: This work is licensed under a Creative Commons Attribution-NonCommercial-NoDerivs 3.0 Unported License. To view a copy of this license, visit http://creativecommons.org/licenses/by-nc-nd/3.0/

How to cite this article: Kuno, A. *et al.* A serum "sweet-doughnut" protein facilitates fibrosis evaluation and therapy assessment in patients with viral hepatitis. *Sci. Rep.* **3**, 1065; DOI:10.1038/srep01065 (2013).

EXPERIMENTAL CELL RESEARCH 319 (2013) 35–44

Available online at www.sciencedirect.com

SciVerse ScienceDirect

journal homepage: www.elsevier.com/locate/yexcr

Research Article

Involvement of hepatocellular carcinoma biomarker, cyclase-associated protein 2 in zebrafish body development and cancer progression

Kathryn Effendi[a], *Ken Yamazaki*[a], *Taisuke Mori*[a], *Yohei Masugi*[a], *Shinji Makino*[b], *Michiie Sakamoto*[a,*]

[a]*Department of Pathology, School of Medicine, Keio University, 35 Shinanomachi, Shinjuku-ku, Tokyo 160-8582, Japan*
[b]*Department of Regenerative Medicine and Advanced Cardiac Therapeutics, Center for Integrated Medical Research, School of Medicine, Keio University, Tokyo, Japan*

ARTICLE INFORMATION

Article Chronology:
Received 20 April 2012
Received in revised form
20 August 2012
Accepted 10 September 2012
Available online 27 September 2012

Keywords:
Skeletal muscle
Actin
Cancer
Development
HCC cells
Zebrafish

ABSTRACT

Cyclase-associated protein 2 (CAP2) is a conserved protein that is found up-regulated in hepatocellular carcinoma (HCC). By using zebrafish, combined with HCC cell lines, we further investigated the role of CAP2. The zebrafish CAP2 sequence was 60% identical to human CAP2 with 77% homology in the C-terminal actin-binding domain, and 58% in the N-terminal cyclase-binding domain. CAP2 expression was observed during zebrafish development and was preferentially expressed in the skeletal muscle and heart. Knockdown using two different morpholinos against CAP2 resulted in a short-body morphant zebrafish phenotype with pericardial edema. CAP2 was observed co-localized with actin in zebrafish skeletal muscle, and in the leading edge of lamellipodium in HCC cell lines. CAP2 silencing resulted in a defect in lamellipodium formation and decreased cell motility in HCC cell lines. Strongly positive expression of CAP2 was observed in 10 of 16 (63%) poorly, 30 of 68 (44%) moderately, and 2 of 21 (10%) well differentiated HCC. CAP2 expression was significantly associated with tumor size, poor differentiation, portal vein invasion, and intrahepatic metastasis. Our results indicate that an important conserved function of CAP2 in higher vertebrates may be associated with the process of skeletal muscle development. CAP2 also played an important role in enhancing cell motility, which may promote a more invasive behavior in the progression of HCC. These findings highlight the link between development and cancer.

© 2012 Elsevier Inc. All rights reserved.

Introduction

Hepatocellular carcinoma (HCC) is the sixth most common malignancy in the world and ranks as the third highest cause of cancer-related death globally [1]. HCC is characterized by an obvious multistage process of tumor development, and as with other cancers, diagnosis of early stage HCC is important for appropriate treatment. Previously, we reported that the cyclase-associated protein 2 (CAP2) gene was upregulated in early HCC [2]. CAP was originally identified in the budding yeast, *Saccharomyces cerevisiae*,

*Corresponding author. Fax: +81 3 3353 3290.
E-mail address: msakamot@z5.keio.jp (M. Sakamoto).

0014-4827/$ - see front matter © 2012 Elsevier Inc. All rights reserved.
http://dx.doi.org/10.1016/j.yexcr.2012.09.013

as a factor required for RAS-activated adenylate cyclase activity [3,4], and since then, at least two homologs of CAP, CAP1 and CAP2 have been found in mammals [5–8]. In yeast, the amino (N)-terminal domain of CAP interacts with adenylyl cyclase and is necessary for the cellular response to activate RAS protein. The carboxyl (C)-terminal domain, on the other hand, appears to play a role in nutritional responses and actin distribution, and is necessary for normal cellular morphology [9–11]. Comparing human or rat CAP protein with yeast indicates that only the C-terminal functions of CAP are highly conserved [5,7]. However, the mechanisms underlying actin regulation by CAP are not yet completely understood. The conservation of CAP functional properties in mammals or higher vertebrates suggests that there are still some unrevealed functions of CAP. The CAP homolog, CAP1 is well studied [12,13] compared with CAP2. Interestingly, we found upregulation of CAP2 in early stage HCC [2], and its expression was related to the multistage development of hepatocarcinogenesis [14]. *CAP2* overexpression has not been previously reported in human cancer. Thus, our previous studies indicated an intriguing function of *CAP2* in HCC, as well as in mammals, which requires further exploration.

Recently, the zebrafish (*Danio rerio*) widely used in developmental studies has emerged as a novel vertebrate model to study cancer susceptibility and carcinogenesis, since they offer combined advantages of invertebrate and mammalian models. They have large clutch sizes, and rapid embryonic development. Organogenesis is easy to examine *in vivo* and in real time. High similarities between the histology of normal and malignant zebrafish tissue to that of mouse and human samples has made zebrafish an excellent model system for cancer [15,16]. Also, the ability to perform large-scale 'reverse' genetics using morpholino synthetic anti-sense oligonucleotides which effectively 'knockdown' gene activity in the zebrafish embryo has further popularized their use as a model system [17,18]. The contribution of zebrafish to the cancer field is still growing. Many approaches to induce tumor formation in zebrafish have been established, and non-invasive methods to image tumor development using the transparent adult zebrafish have also recently been developed [19,20]. Thus, zebrafish have now emerged as a new favorite model to study both development and cancer.

In this study, we examined the expression of CAP2 during zebrafish development and utilized morpholino antisense oligonucleotides for protein knockdown studies in zebrafish. We also investigated the functional role of CAP2 using HCC cell lines and further examined CAP2 expression in HCC clinical specimens.

Material and methods

Embryo collection

Zebrafish embryos were obtained by natural mating of RIKEN wild-type zebrafish (*Danio rerio*). Collected embryos were maintained in egg water (5 mM NaCl, 0.17 mM KCl, 0.33 mM $CaCl_2$, 0.33 mM $MgSO_4$, 10^{-5}% methylene blue) at 28.5 °C and embryos were staged using standard morphological criteria [21]. Embryos were gently dechorionated using watchmaker's forceps.

Tissue resection

Adult zebrafish were anesthetized with tricaine (1:20 dilution in clean tank water) and placed on a sponge. Resection was performed under brightfield imaging on a dissection microscope. The incision was made through the ventral body wall and posterior to the heart using microdissection scissors. The brain, eye, heart, abdominal organs, and skeletal muscle were resected using forceps and quickly placed in lysis buffer for Western blot analysis, or frozen in liquid nitrogen for RNA extraction.

Morpholinos and microinjections

Morpholino antisense oligonucleotides were obtained from Gene Tools LLC (Oregon, USA). Two non-overlapping CAP2 antisense morpholinos, and each corresponding five-mispair control morpholinos were designed: (A) ATG-MO (5′-GACGACCAACCAGAGCCTCCA-TAAC-3′), with its control (5′-GAgGAgCAACCACCAcAGCCTCgATt-AC-3′) and (B) UTR-MO (5′-ATATTACCTCAGATGGTGTGGCCCG-3′), with its control (5′-ATtTTACCTgAGATcGTGTaGCgCG-3′). The sequence of CAP1 antisense morpholino was as follows: ATG-MO (5′-ATCTGCCATGCCGTCGCCGTGTGAA-3′), with its five-mispair control (5′-ATgTGCgATGCCcTCGCCcTGTcAA-3′). The sequence used for standard control was 5′-CCTCTTACCTCAGTTACAATTTATA-3′. Morpholino oligonucleotides were stored in 1.0 mM concentration and were diluted to working concentrations in 1× Danieau's buffer. A dose range of 0.1–1 mM ATG-MO was defined as effective and specific window of concentration which resulted in comparable specific phenotypes. We used 0.3 mM as our choice of morpholino concentration. For the double knockdown approach, CAP2 and CAP1 morpholinos were mixed in a 1:1 ratio (0.3 mM). Fertilized embryos were injected at the 1–8 cell stages into the cytoplasmic streaming of the yolk with 1–2 nL of solution containing either morpholino, or its mispair control. They were allowed to develop in egg water maintained at 28.5 °C. Developed embryos were photographed using a Leica M275 microscope and further evaluated by Western blot and immunohistochemical analysis.

Western blotting

Lysates of HCC cancer cells, adult male zebrafish organs, and zebrafish larva were gently homogenized in lysis buffer (50 mM Tris–HCl (pH 7.4), 250 mM NaCl, 5 mM EDTA, 1% NP-40 (IGEPAL), 10% glycerol, 1 mM DTT, and 25× protease inhibitor). After determining protein concentrations using the Quant-iT™ Protein Assay Kits (Invitrogen, Eugene, OR), lysates were loaded onto and separated on SDS-PAGE (4–12% Bis-Tris gel; Invitrogen, Carlsbad, CA), and transferred to PVDF membrane using the semi-dry blotting method. The membranes were blocked with 5% nonfat dry milk and probed with our originally raised rabbit polyclonal antibodies against human CAP2 (1/500), CAP1 (1/200) [14], and a mouse monoclonal beta actin antibody (1/1000; Sigma-Aldrich, St. Louis, MO, USA) as a loading control. Horseradish peroxidase-conjugated secondary antibodies were used to probe the membranes and visualized with ECL western blotting detection reagents (GE Healthcare, UK Ltd., Buckinghamshire, UK).

Immunohistochemical analysis

Zebrafish specimens were fixed in 4% paraformaldehyde-PBS at 4 °C overnight and embedded in paraffin tissue section. For staining, slides were deparaffinized and rehydrated, and sections were heated at 120 °C in 0.1 mM Tris–HCl buffer (pH 9.0) for 10 min using an autoclave. The sections were incubated with

rabbit anti-human CAP2 (1/4000), and CAP1 (1/2000), followed by ImmPRESS anti-rabbit Ig Kit secondary antibody (Vector Laboratories, Burlingame, CA). A rabbit immunoglobulin (1/50000; DAKO X0936, Glostrup, Denmark) was used as a negative control. The sections were counterstained with hematoxylin and then mounted. Immunohistochemical staining for HCC clinical specimens was done on formalin-fixed, paraffin-embedded tissue sections according to the methods previously described [14]. Staining analysis was done at least twice. Smooth muscle of the vascular wall served as the internal positive control. We defined CAP2 staining criteria as follows: intensity stronger than or equal to the positive control with more than 50% positive cell in each lesion was scored 2+, while less than 50% positive cell was scored 1+; intensity weaker than the positive control with positive cell more than 50% was also scored 1+, and with positivity less than 50% was considered negative. According to the previous result of CAP2 expression in HCC [14], we used 50% as a cut-off value to divide the HCC cases into high and low positivity group.

Tissue specimens of HCC

HCCs and corresponding non-cancerous liver tissue were obtained from 91 patients with 105 nodules (21 well differentiated (including 9 early), 68 moderately differentiated, and 16 poorly differentiated HCCs) who underwent surgical resection at Keio University Hospital (Tokyo, Japan) between 2003 and 2006. The histological diagnosis was made according to the criteria set by the World Health Organization [22]. This study was approved by the Ethics Committee of Keio University School of Medicine.

Cell culture

The human HCC cell line, PLC/PRF/5, was obtained from the American Type Culture Collection (Manassas, VA). KYN-2 was established as reported previously [23]. All the cells were grown in RPMI 1640 medium supplemented with 10% fetal bovine serum, 100 U/mL penicillin, and 100 μg/mL streptomycin.

Immunocytochemical analysis

PLC/PRF/5 and KYN-2 cells were grown to confluence on glass slides, fixed with 3.7% formaldehyde, and permeabilized with 0.1% Triton X-100 in phosphate buffered saline. The slides were incubated overnight at 4 °C with CAP2 antibody (1/100). After rinsing, the slides were covered with FITC-labeled secondary antibody (Dako, Glostrup, Denmark) with rhodamine-phalloidin and Hoechst 33342 dye (Invitrogen), and visualized using an Axiovert 200 microscope, and AxioCam CCD camera (Carl Zeiss MicroImaging Inc., Tokyo, Japan). For negative control, PLC/PRF/5 was incubated without primary antibody, and visualized using the LSM 510 Meta confocal microscope (Carl Zeiss, Oberkochen, Germany). All staining analysis was done at least twice.

RNA interference and serum stimulation analysis

Two small interfering RNA (siRNA) targeting two CAP2 sequence (siCAP2A and siCAP2B) were synthesized by B-Bridge International, Inc. The target sequences were GGAGUGAACUUCAAGCAUA and GGAGUUGGAAGGAAAGAAA. Cells were cultured until 70–80% confluence onto collagen I-coated six-well plates, and were transfected with siRNA using the DharmaFECT General Transfection Protocol (Dharmacon, Thermo Fisher Scientific, Lafayette, CO, USA). A non-targeting siRNA pool (QIAGEN, Valencia, CA, USA) was used as a negative control. Cells were incubated at 37 °C, 5% CO_2 for 48 h, and to observe lamellipodium formation, the transfectants were serum starved for 24 h. On the following day, the serum was changed with medium supplemented with 10% FBS for 30 min.

Semi-quantitative RT-PCR analysis

Purification of RNA from each zebrafish tissue samples was accomplished by isolation through Isogen (Nippon Gene Co. LTD, Toyama, Japan), and cDNA was synthesized using the PrimeScript RT reagent Kit (Takara Bio, Shiga, Japan). As a template for amplification, 10 μL of each sample was used. A primer set designed for zebrafish CAP2 expression amplified a 175 base pair fragment (5′-GGCTGATTGATCTGCCTCCTC-3′ and 5′-AAGCACAGTGGGTCTGGGG-3′), and a primer set targeting zebrafish CAP1 amplified a 179 base pair fragment (5′-GATGGCTGCCACGTGTACCT-3′ and 5′-ATCTCGGTGGCTGTGGTGAC-3′). Each reaction was run on 2% agarose in 1 × TAE buffer.

Migration assay

PLC/PRF/5 and KYN-2 cells transfected for 48 h with siCAP2A, siCAP2B, and negative control siRNA were suspended in medium supplemented with 0.5% FBS. Cells treated with each siRNA were dispersed in each of three independent upper chambers of BD BioCoat Control Culture Inserts (pore size=8 μm; BD Biosciences, San Diego, CA, USA). Chemoattractant medium containing 10% FBS was added to the bottom plate. After 24 h incubation, non-migrated cells were removed by scrubbing with cotton-tipped swabs and migrated cells were stained with Diff-Quick stain (Kokusai Shiyaku, Kobe, Japan). The number of migrated cells on three independent membranes was counted under microscope. The ratio of the number of migrated cells represents the mean number of migrated cells with each siRNA treatment, divided by the mean number of migrated control cells.

Statistical analysis

The chi-squared test was used when appropriate to determine the correlations between clinicopathological variables and CAP2 expression. Statistical significance was defined as $P<0.005$. All statistical analyses were carried out using SPSS statistical software (SPSS, Chicago, IL, USA).

Results

CAP2 is expressed in both the embryo and adult zebrafish

The conservation of CAP2 from yeast to mammals suggests that CAP2 also exists in zebrafish. We examined CAP2 presence in zebrafish and found that the zebrafish Cap2 sequence (LOC393809; NP_957130.1) was 60% identical to the already known human CAP2, with 77% homology in the C-terminal actin-binding domain, 57% in the middle proline-rich sequence, and 59% in the N-terminal

domain (Fig. 1A). Although all three domains of CAP were conserved, homologies in the C-terminal actin-binding domain were higher than other regions. By immunohistochemical analysis, CAP2 expression could be observed in 24 h post-fertilization (hpf) embryo, and continued in the larva and adult zebrafish. In the early embryo development (Fig. 1B), CAP2 was seen in the neural tube (nt), and a group of tissues that will give rise to a muscle segment, the myotome (my). As the embryo developed to larva, CAP2 expression was observed in the brain (br), and skeletal muscle (sk). In adult zebrafish tissue, CAP2 expression was also observed in the brain, heart and skeletal muscle (Fig. 1C and D). We also compared the expression of CAP2 and CAP1, a homolog of CAP2 that also has been identified in zebrafish [24,25]. Differential expression of CAP2 was particularly observed in the heart and skeletal muscle, where CAP2 was highly expressed (Supplementary Fig. 1A).

CAP2 zebrafish morphants showed an abnormal short-body phenotype

To study CAP2 function in zebrafish, we created CAP2 knockdown morphants by injecting CAP2 antisense morpholino oligonucleotides into cytoplasmic streaming of 1- to 8-cell stage zebrafish embryos. To assess specificity, two non-overlapping morpholinos (A and B) were designed against a CAP2 sequence, with five-mispair control oligo for each morpholino as a negative

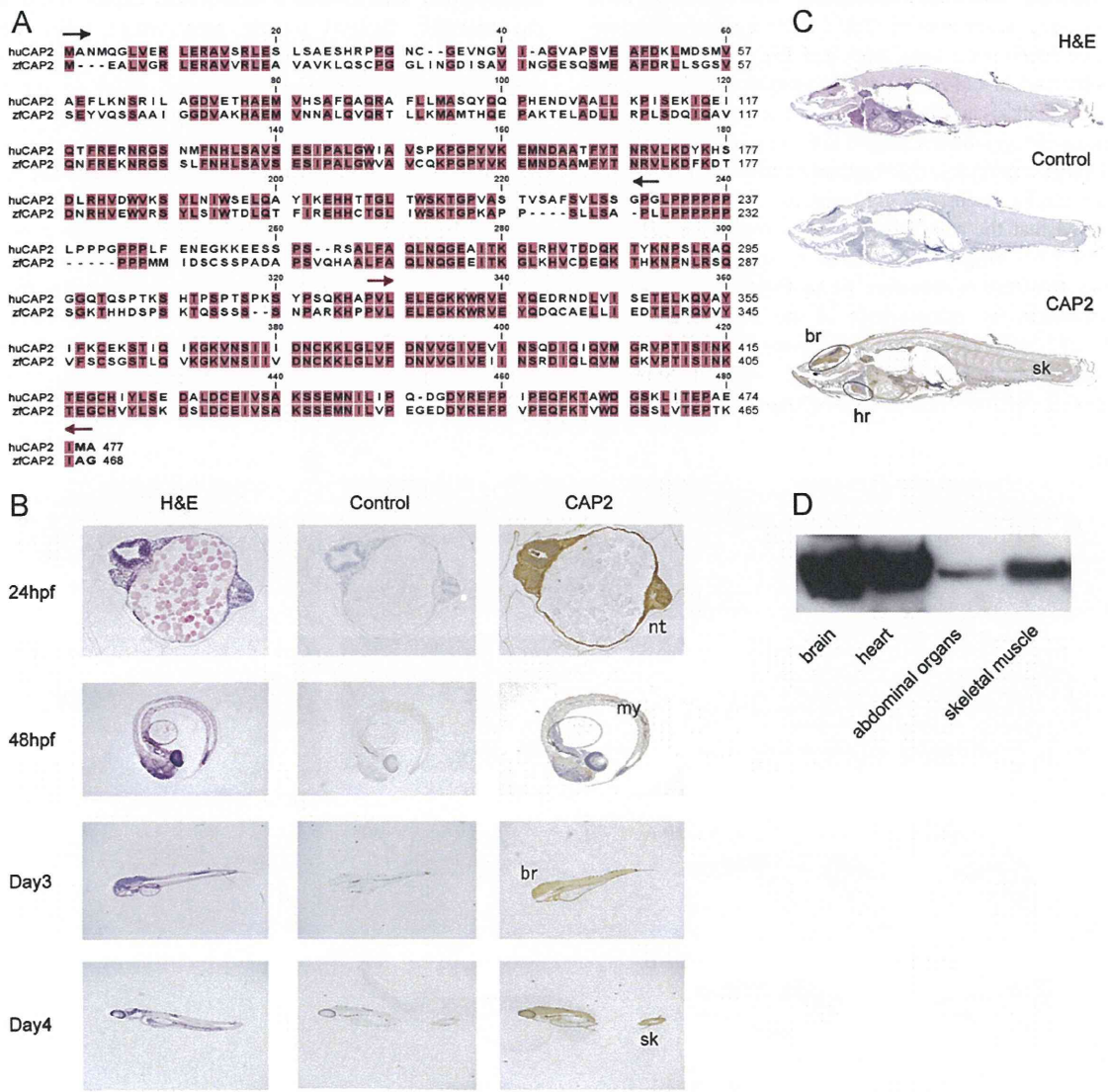

Fig. 1 – Cyclase-Associated Protein 2 (CAP2) is expressed in both embryo and adult zebrafish. (A) Direct amino acid comparison between human and zebrafish CAP2 sequences, with conserved amino acids highlighted in red. The N-terminal domain is depicted by black arrows, C-terminal domain is depicted by red arrows, and between them is a proline-rich sequence. (B) CAP2 expression in zebrafish embryo, 24 and 48 hpf, followed by day 3 and day 4 larva. CAP2 was expressed in the neural tube (nt) and in the myotome (my) of a 48 hpf embryo. In day 3 and day 4 larva, CAP2 was expressed in the brain (br) and skeletal muscle (sk). (C) CAP2 expression in adult male zebrafish was observed in the brain, heart (hr) and skeletal muscle. Negative control was included in each staining. (D) Protein expression was confirmed with Western blot analysis. (For interpretation of the references to color in this figure legend, the reader is referred to the web version of this article.)

control. Injecting either CAP2 morpholinos resulted in reproducible and identical morphants phenotypes. In 24 hpf, we observed that most of the morphants embryos (MO A, B) showed shorter body length compared with the mispaired control (MP A, B) (Fig. 2A). Additional controls using tracer injected embryos (PR) as well as wild-type embryos (WT) did not show an abnormal phenotype (Fig. 2A). CAP2 morphant embryos also displayed pericardial edema with persistently short-body phenotype at three days post-fertilization, while the mispair control embryos developed similarly to the wild-type (Fig. 2B). To make sure that the experiment is being performed in the effective and specific concentration range, injection of the CAP2 targeted morpholino was performed side-by-side with the five-mispair control oligo, and the resulting short-body phenotype was observed in a concentration-dependent manner (Table 1). At least two independent injection experiments were replicated. Reduced CAP2 expression was observed in CAP2 knockdown morphant embryos with immunohistochemical analysis (Fig. 2C). The morphants were mostly non-motile and did not survive due to stalled development. Additional control using 0.3 mM standard control oligo which has been known can be extensively used without triggering off-target effects showed that the resulting short-body phenotype could be reduced until 17% (Supplementary Table 1). Since CAP1 was also ubiquitously expressed in zebrafish, we performed double knockdown experiments by mixing both of the two sequences of CAP2 and CAP1 morpholinos. Similar short-body phenotype was observed, and a clear reduction of both CAP2 and CAP1 expression was obtained in Western blot analysis (Supplementary Fig. 1B). The number of morphant short-body embryos was not enhanced by the double knockdown strategy (Table 1), suggesting no interference between each other.

CAP2 colocalized with actin both in zebrafish and HCC cell lines

Both CAP2 and CAP1 protein were detected from the zebrafish larval period, however, clear strong expression of CAP2 was particularly observed in the skeletal muscle area, while only thin weak expression of CAP1 was observed in the same area of skeletal muscle. Immunostaining using antibody against muscle actin and alpha-sarcomeric actin, i.e., it only reacts with skeletal muscle actin, also showed a strong clear expression of actin in the zebrafish skeletal muscle area, where CAP2 was also expressed. They both showed a similar expression pattern suggesting colocalization of CAP2 and actin in the skeletal muscle of zebrafish (Fig. 3A, Supplementary Fig. 1C). These findings indicate the possibility that the abnormal short-body phenotype seen in the CAP2 zebrafish morphants may be due to the downregulation of actin-associated CAP2. We also investigated colocalization of CAP2 and actin in human cancer cells. According to our previous report, CAP2 was highly expressed in multistage hepatocarcinogenesis, and we frequently found that the tumor cells invading the stroma were clearly stained with CAP2 [14]. In the present study, we found that CAP2 was highly distributed in the perinuclear area, and was also co-localized with actin in the leading edge of lamellipodium in PLC/PRF/5, and

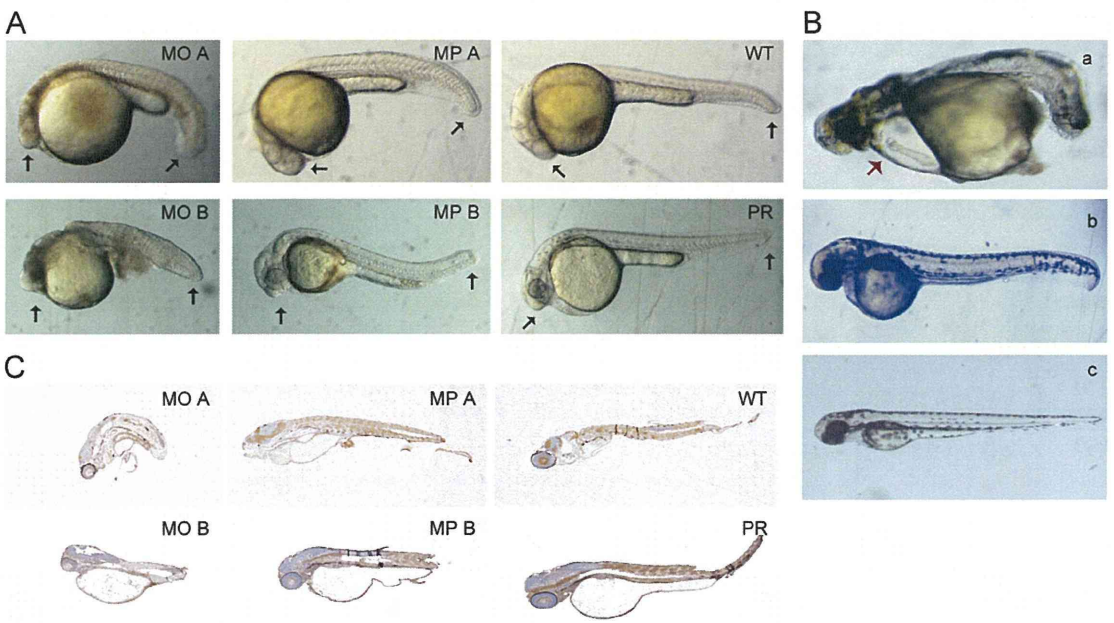

Fig. 2 – Cyclase-associated protein 2 (CAP2) zebrafish morphants showed a short-body phenotype. (A) Shorter body length was observed in morphant-A and morphant-B CAP2 embryos (MO A, MO B) compared with each five-mispair negative control (MP A, MP B), wild-type control (WT), and additional injection controls using embryos injected only with the tracer, phenol red (PR). Black arrows mark the length boundary. (B) The resulting short-body phenotype was persistently observed with pericardial edema (red arrow) at 3 days post fertilization (a), while developmental defects were not observed in morphant controls (b) or wild-type embryos (c). All morphants were injected with 0.3 mM concentration of morpholino. (C) At 5 days post fertilization, immunohistochemical analysis showed reduced expression of CAP2 in both morphants, compared with the mispair controls and wild-type or tracer control embryos. (For interpretation of the references to color in this figure legend, the reader is referred to the web version of this article.)

Table 1 – Concentration-dependence effect of cyclase-associated protein2 (CAP2) morpholinos on early development of zebrafish embryos.

Injections	Embryos injected	Eggs left after 24 h	Normal	Short-body	Percentage showing phenotype
0.1 mM (MO-A)[a]	59	52	41	11	21
0.1 mM (MP-A)[b]	68	61	56	5	8
0.3 mM (MO-A)	154	78	12	66	85
0.3 mM (MP-A)	94	37	25	12	32
0.5 mM (MO-A)	82	35	3	32	91
0.5 mM (MP-A)	86	41	26	15	37
1 mM (MO-A)	118	10	3	7	70
1 mM (MP-A)	120	55	15	40	73
0.3 mM (MO-B)[c]	68	60	3	57	95
0.3 mM (MP-B)[d]	69	62	55	7	11
CAP2A+ CAP1 (MO)	59	26	2	24	92
CAP2A+CAP1 (MP)	83	54	19	35	65
CAP2B+CAP1 (MO)	75	56	7	49	88
CAP2B+CAP1 (MP)	76	54	39	15	28

[a] Antisense morpholino A.
[b] Mispaired control A.
[c] Antisense morpholino B.
[d] Mispaired control B.

the highly metastatic, KYN-2, HCC cell lines (Fig. 3B, Supplementary Fig. 2). These findings suggest that the role of CAP2 in inducing stromal invasion may relate to its actin cytoskeletal function.

CAP2 silencing in HCC cell lines resulted in a defect in lamellipodium formation and a reduction in cell motility

We further assessed the role of CAP2 in relation to its cytoskeletal function. CAP2 knockdown was performed in HCC cell lines using two small interfering RNA molecules (siCAP2 A and siCAP2B). The knockdown effect was confirmed using Western blot analysis (Fig. 4A), and the transfected cells were serum starved for 24 h before stimulation with serum the next day. Within 15 min after serum stimulation, control cells started to spread out and extended lamellipodium around the circumference of the cell clusters. Lamellipodium formation in CAP2-knockdown cells was, however, still restrained or only partial (Fig. 4B). The role of CAP2 in cell motility was evaluated by migration assay with CAP2-knockdown cells. The number of migrating CAP2-knockdown cells decreased compared with the controls (Fig. 4C). We did not observe reduced cell proliferation in CAP2-knockdown cells (data not shown), suggesting that the decreased number of migrated cells was solely due to the reduced cell motility caused by CAP2 knockdown.

CAP2 expression in HCC clinical cases correlated with tumor size, poor differentiation, portal vein invasion, and intrahepatic metastasis

We evaluated CAP2 expression in 105 HCC nodules (21 well differentiated (including 9 early), 68 moderately differentiated, and 16 poorly differentiated HCCs). Immunohistochemical evaluation was done by combining the intensity and positivity of CAP2 staining (Supplementary Fig. 3). Strongly positive expression of CAP2 was mostly observed in progressed HCC. A 2+ score was observed in 10 of the 16 (63%) poorly differentiated HCCs, 30 of the 68 (44%) moderately differentiated HCCs, and 2 of the 21 (10%) well differentiated HCCs (none of the early nodules had 2+ score). Reversely, negative expression was observed in only 2 of the 16 (13%) poorly differentiated HCCs, 3 of the 68 (4%) moderately differentiated HCCs, and 10 of the 21 (48%) well differentiated HCCs (including 6 of the 9 early nodules (67%)) (Table 2). CAP2 expression was significantly associated with tumor size ($P=0.004$), poor differentiation ($P=0.001$), portal vein invasion ($P=0.001$), and intrahepatic metastasis ($P=0.002$) (Table 3).

Discussion

Cyclase-associated protein, CAP, has been identified as a bifunctional protein from yeast through mammals, indicating the retention of important conserved functions during evolution. A homolog of yeast CAP, which is required for proper genesis of cell polarity in eukaryotes, has been identified in *Drosophila*. Loss of *Drosophila* CAP causes cell polarity defects, altering the distribution of actin filaments and resulting in various developmental defects [26]. CAP knockout mutant *Dictyostelium* cells showed changes in cell polarity, F-actin organization, and phototaxis suggesting that CAP may play a critical part in cell polarity and movement of diverse organisms [27]. In human and adult rat tissue, at least two different homologs of CAP, CAP1 and CAP2, have been found, and they share more than 60% amino acid identity [5,6,8]. However, the functions of CAPs in mammals or higher vertebrates are not well established, and in particular, studies on CAP2 are lacking. In the zebrafish, the gene encoding CAP1 has been reported and shares 63% identity with human CAP1 [24]. In the present study, we identified a CAP2 protein which shares 60% identity with human CAP2. Although both CAPs are conserved in zebrafish, their expression pattern is different. We observed that CAP2 was expressed in the brain,

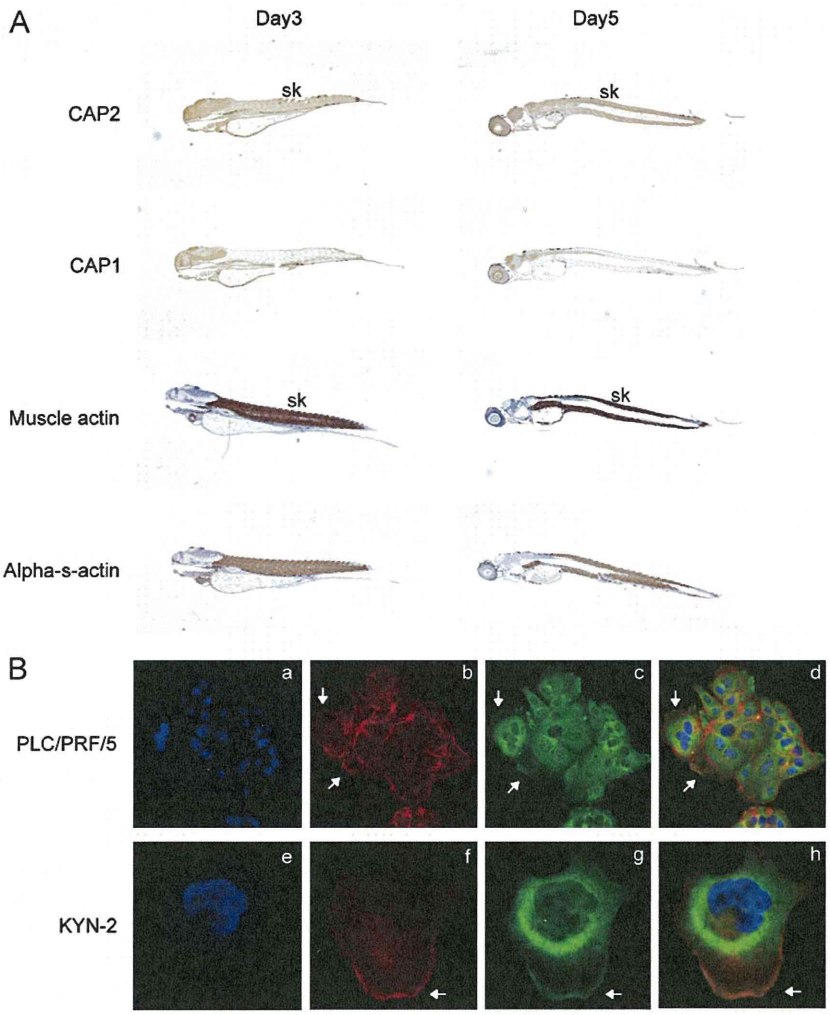

Fig. 3 – Cyclase-associated protein 2 (CAP2) observed co-localized with actin in zebrafish and hepatocellular carcinoma (HCC) cell lines. (A) Day 3 and day 5 of zebrafish larva with CAP2, CAP1 and actin immunostaining. CAP2 was highly expressed in the skeletal muscle area compared with CAP1. Immunostaining of muscle actin and alpha-sarcomeric actin was also observed in the zebrafish skeletal muscle area, suggesting co-localization of skeletal muscle actin and CAP2, magnification 20 ×. (B) Immunocytochemistry of PLC/PRF/5 and KYN-2 HCC cell lines. CAP2 expression was observed co-localized with the lamellipodium as a characteristic feature of motile cells, marked by white arrow (a,e, Hoechst: blue; b,f, anti-phalloidin-rhodamine: red; c,g, anti-CAP2: green; d,h, merged). (For interpretation of the references to color in this figure legend, the reader is referred to the web version of this article.)

and was particularly expressed in the heart and skeletal muscle. This is in accordance with previous reports showing that CAP1 is widely expressed in nearly all organs, while CAP2 expression is localized in the brain, heart, and skeletal muscle in rat tissue [8,28]. In mouse embryonic development, the expression of CAP2 is highly restricted to the developing muscle tissues and heart [12]. A new report has shown CAP2 expression in the cardiac primordial and in the leading edge of the myotome during early *Xenopus* embryogenesis [29]. We found that knockdown of CAP2 expression in the zebrafish resulted in a shorter body compared with the control embryos. There was an abundant original expression and a co-localization of CAP2 and actin in the zebrafish skeletal muscle. CAP2 appears to act as a striated muscle-specific protein during zebrafish development. Thus, the short-body phenotype with pericardial edema observed after CAP2 knockdown in zebrafish was likely caused by the down regulation of actin-associated CAP2. This indicates that CAP2 plays an important conserved role in higher vertebrates, particularly in the development of skeletal muscle. We realized that almost all knockdowns of various genes in zebrafish affect body development [30–32], through skeletal muscle, somite, or neural formation defects, indicating that many genes or signaling pathways are involved in the patterning processes in a vertebrate embryo; here we showed the possible role of CAP2. Further, it would be interesting to investigate the mechanisms regulating CAP2 and CAP1 in developmental processes and in different organs.

Previously, using oligonucleotides array technology we identified *CAP2* as one of the genes upregulated in early HCC [2]. Overexpression of CAP2 was observed in a stepwise manner

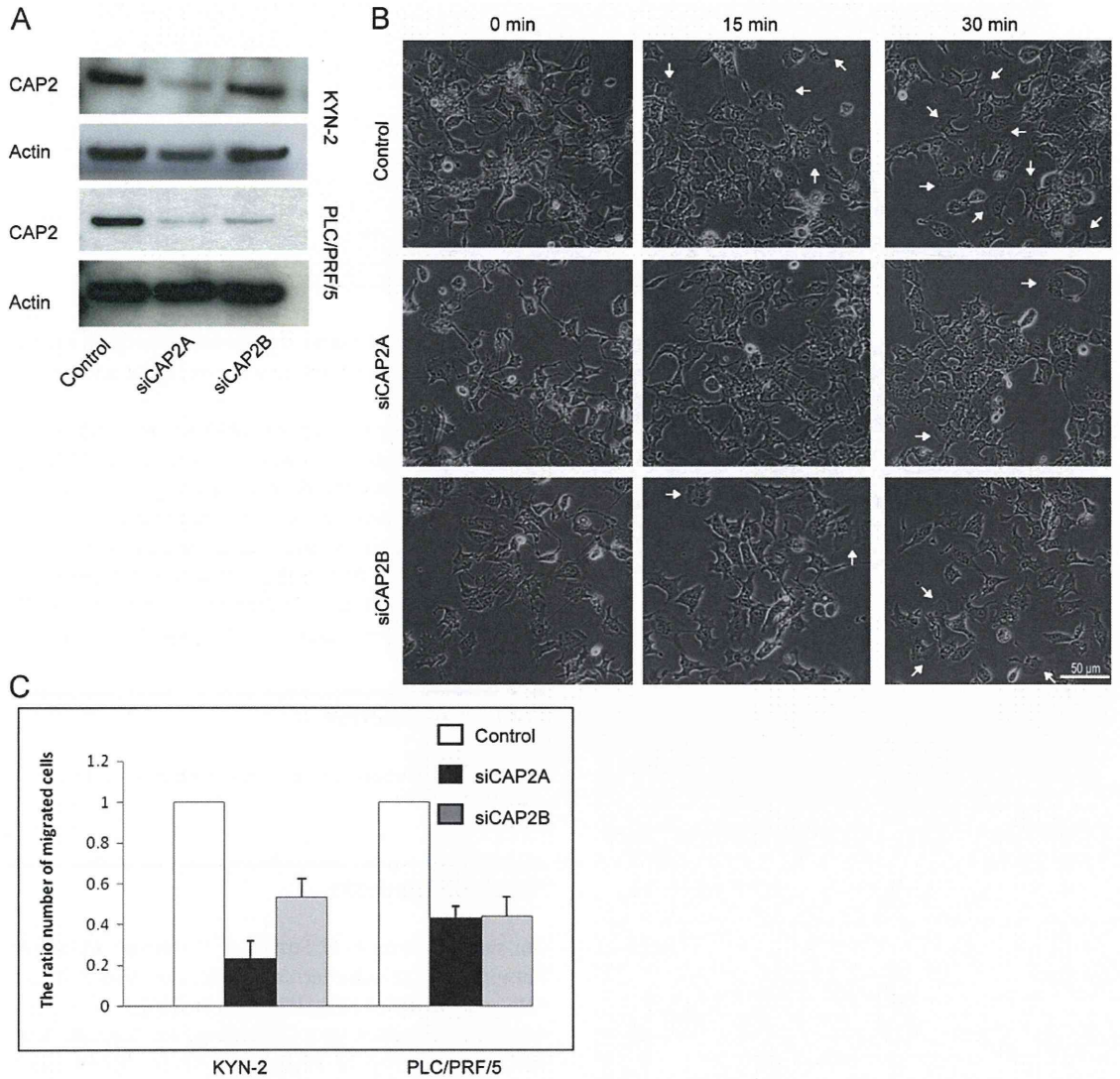

Fig. 4 – Cyclase-associated protein 2 (CAP2) silencing affected lamellipodium formation and cell migration. (A) Western blot analysis to confirm the suppression of CAP2 in KYN2 and PLC/PRF/5 cell lines. (B) Serum stimulation analysis of KYN-2 cells. After serum-starving (0 min), the lamellipodium of control cells was soon established following serum-stimulation (15 and 30 min) compared with the CAP2-knockdown cells, siCAP2A and siCAP2B. White arrows indicated the lamellipodium formation. Scale bar=50 μm. (C) Migration assay showing a reduction in the migration of both KYN-2 and PLC/PRF/5 cells, compared with the control cells. The ratio of the number of migrated cells represents the mean number (under microscope observation) of migrated cells per field against control cells. Bars reveal standard error of the mean (SEM).

during the progression of HCC and interestingly, in early HCC, the tumor cells invading the stroma stained positive for CAP2 and were clearly highlighted [14]. Here, we further investigated the co-localization of CAP2 and actin in the leading edge of the lamellipodium of HCC cells. Extension of the lamellipodium following serum stimulation was inhibited, and cell motility was reduced in CAP2 knockdown cells. This suggests CAP2 involvement in remodeling of the actin filament that occurs at the leading edge of lamellipodium as a characteristic feature of motile cells. The polymerization of actin is essential for motile processes and is regulated by some signaling pathway for actin-binding protein [33,34]. Thus, CAP2 seems to play a role in cell motility, resulting in promoting skeletal muscle development, and stromal invasion in early HCC. Moreover, we observed a significant correlation between overexpression of CAP2 and progressed features in HCC, such as tumor size, poor differentiation, portal vein invasion, and intrahepatic metastasis. This suggests that CAP2 overexpression is involved in promoting the invasive behavior of HCC cells. The role of CAP2 in other human cancers is, however, not yet clear. Human CAP2 can also interact with CAP1 and actin [35]. We have reported that the overexpression of CAP1 in pancreatic cancers is also related to the aggressive behavior of pancreatic cancer cells [36]. Further investigation of cellular and molecular mechanisms governing CAP2 role in cell migration ability is necessary to expand our knowledge on how actin dynamics is controlled. Elucidating the

Table 2 – Immunohistochemical analysis of cyclase-associated protein (CAP2) in hepatocellular carcinoma (HCC) (n=105).

Histology	CAP2 staining score		
	2+	1+	–
Well differentiated HCC (n=21)	2(10%)	9(43%)	10(48%)
Early HCC (n=9)	0(0%)	3(33%)	6(67%)
Moderately differentiated (n=68)	30(44%)	35(51%)	3(4%)
Poorly differentiated (n=16)	10(63%)	4(25%)	2(13%)

Table 3 – Correlations between clinicopathological characteristics and cyclase-assoicated protein 2 (CAP2) expression in HCC clinical cases.

Characteristics	CAP2 expression		
	–, 1+	2+	*P* value
Mean age (years)			NA[a]
Gender			0.810
Male	51	36	
Female	10	8	
Etiology			
Hepatitis B virus			0.010
Negative	51	27	
Positive	10	17	
			0.052
Negative	23	25	
Positive	38	19	
AFP serum level (ng/ml)			0.492
<20	36	23	
≧20	25	21	
Fibrosis			0.073
Liver cirrhosis	24	23	
Others	37	17	
Tumor size (cm)			0.004
<2.0	24	6	
≧2.0	37	38	
Tumor differentiation			0.001
Well (early)	19(9)	2(0)	
Moderately	37	31	
Poorly	5	11	
Portal involvement			0.001
–	37	12	
+	24	32	
Intrahepatic metastasis			0.002
–	53	27	
+	8	17	

[a] Not available.

conserved collaborative role of CAP2 and CAP1, and whether they interact with the RAS signaling pathway may also reveal their role in human cancers. Additionally, the use of zebrafish to study hepatocarcinogenesis offers a new innovative research approach [37]. A previous report has shown conserved gene expression profiles between human and zebrafish liver cancer [38]. Future studies on how CAP2 functions in zebrafish liver are necessary to advance our understanding of hepatocarcinogenesis. Combining developmental and cancer studies will provide an exciting future framework to understand how development and carcinogenesis are linked.

In summary, we showed that CAP2 has an important conserved function across species. In zebrafish, the role of CAP2 appears to be associated with the developmental process, particularly in skeletal muscle development. In HCC, CAP2 was associated with enhanced cell motility, and was involved in the progression of HCC. The role of CAP2 in the developmental process of higher vertebrates as well as in human liver cancer is shedding some light on the progress issue of development and cancer.

Conflict of interest

The authors declare there is no conflict of interest regarding this study.

Acknowledgments

Our sincere thanks to H. Suzuki, Y. Hashimoto, M. Suzuki, and K. Nakajima, for providing technical assistance. Also, to M. Ono for her help and support at Keio University Small Fish Center (KSFC). This work was supported by a Grant-in-aid for Scientific Research (B) from the Ministry of Education, Culture, Sports, Science, and Technology (MEXT) of Japan; Grants for the Health Labor Sciences Research and the Third Term Comprehensive 10-Year Strategy for Cancer Control from the Ministry of Health, Labor and Welfare of Japan; Grant-in-aid from The Vehicle Racing Commemorative Foundation. This study was performed as a research program of the Project for Development of Innovative Research on Cancer Therapeutics (P-Direct) from the Ministry of Education, Culture, Sports, Science and Technology of Japan.

Appendix A. Supporting information

Supplementary data associated with this article can be found in the online version at http://dx.doi.org/10.1016/j.yexcr.2012.09.013.

REFERENCES

[1] D.M. Parkin, F. Bray, J. Ferlay, P. Pisani, Global cancer statistics, 2002, CA Cancer J. Clin. 55 (2005) 74–108.
[2] M. Chuma, M. Sakamoto, K. Yamazaki, T. Ohta, M. Ohki, M. Asaka, S. Hirohashi, Expression profiling in multistage hepatocarcinogenesis: identification of HSP70 as a molecular

marker of early hepatocellular carcinoma, Hepatology 37 (2003) 198–207.
[3] J. Field, A. Vojtek, R. Ballester, G. Bolger, J. Colicelli, K. Ferguson, J. Gerst, T. Kataoka, T. Michaeli, S. Powers, M. Riggs, L. Rodgers, I. Wieland, B. Wheland, M. Wigler, Cloning and characterization of CAP, the *S. cerevisiae* gene encoding the 70 kd adenylyl cyclase-associated protein, Cell 61 (1990) 319–327.
[4] M. Fedor-Chaiken, R.J. Deschenes, J.R. Broach, SRV2, a gene required for RAS activation of adenylate cyclase in yeast, Cell 61 (1990) 329–340.
[5] H. Matviw, G. Yu, D. Young, Identification of a human cDNA encoding a protein that is structurally and functionally related to the yeast adenylyl cyclase-associated CAP proteins, Mol. Cell. Biol. 12 (1992) 5033–5040.
[6] G. Yu, J. Swiston, D. Young, Comparison of human CAP and CAP2, homologs of the yeast adenylyl cyclase-associated proteins, J. Cell Sci. 107 (Pt 6) (1994) 1671–1678.
[7] A. Zelicof, J. Gatica, J.E. Gerst, Molecular cloning and characterization of a rat homolog of CAP, the adenylyl cyclase-associated protein from *Saccharomyces cerevisiae*, J. Biol. Chem. 268 (1993) 13448–13453.
[8] J. Swiston, A. Hubberstey, G. Yu, D. Young, Differential expression of CAP and CAP2 in adult rat tissues, Gene 165 (1995) 273–277.
[9] J.E. Gerst, K. Ferguson, A. Vojtek, M. Wigler, J. Field, CAP is a bifunctional component of the *Saccharomyces cerevisiae* adenylyl cyclase complex, Mol. Cell. Biol. 11 (1991) 1248–1257.
[10] A. Vojtek, B. Haarer, J. Field, J. Gerst, T.D. Pollard, S. Brown, M. Wigler, Evidence for a functional link between profilin and CAP in the yeast *S. cerevisiae*, Cell 66 (1991) 497–505.
[11] F. Shima, T. Okada, M. Kido, H. Sen, Y. Tanaka, M. Tamada, C.D. Hu, Y. Yamawaki-Kataoka, K. Kariya, T. Kataoka, Association of yeast adenylyl cyclase with cyclase-associated protein CAP forms a second Ras-binding site which mediates its Ras-dependent activation, Mol. Cell. Biol. 20 (2000) 26–33.
[12] E. Bertling, P. Hotulainen, P.K. Mattila, T. Matilainen, M. Salminen, P. Lappalainen, Cyclase-associated protein 1 (CAP1) promotes cofilin-induced actin dynamics in mammalian nonmuscle cells, Mol. Biol. Cell 15 (2004) 2324–2334.
[13] K. Moriyama, I. Yahara, Human CAP1 is a key factor in the recycling of cofilin and actin for rapid actin turnover, J. Cell Sci. 115 (2002) 1591–1601.
[14] R. Shibata, T. Mori, W. Du, M. Chuma, M. Gotoh, M. Shimazu, M. Ueda, S. Hirohashi, M. Sakamoto, Overexpression of cyclase-associated protein 2 in multistage hepatocarcinogenesis, Clin. Cancer Res. 12 (2006) 5363–5368.
[15] J.F. Amatruda, J.L. Shepard, H.M. Stern, L.I. Zon, Zebrafish as a cancer model system, Cancer Cell 1 (2002) 229–231.
[16] W. Goessling, T.E. North, L.I. Zon, New waves of discovery: modeling cancer in zebrafish, J. Clin. Oncol. 25 (2007) 2473–2479.
[17] A. Nasevicius, S.C. Ekker, Effective targeted gene 'knockdown' in zebrafish, Nat. Genet. 26 (2000) 216–220.
[18] D.R. Corey, J.M. Abrams, Morpholino antisense oligonucleotides: tools for investigating vertebrate development, Genome Biol. 2 (2001) (REVIEWS1015).
[19] K. Stoletov, R. Klemke, Catch of the day: zebrafish as a human cancer model, Oncogene 27 (2008) 4509–4520.
[20] R.M. White, A. Sessa, C. Burke, T. Bowman, J. LeBlanc, C. Ceol, C. Bourque, M. Dovey, W. Goessling, C.E. Burns, L.I. Zon, Transparent adult zebrafish as a tool for in vivo transplantation analysis, Cell Stem Cell 2 (2008) 183–189.
[21] C.B. Kimmel, W.W. Ballard, S.R. Kimmel, B. Ullmann, T.F. Schilling, Stages of embryonic development of the zebrafish, Dev. Dyn. 203 (1995) 253–310.
[22] S. Hirohashi, K. Ishak, M. Kojiro, I. Wanless, N.D. Theise, H. Tsukuma, Tumours of the liver and intrahepatic bile ducts, in: S.R. Hamilton, L.A. Aaltonen (Eds.), Pathology and Genetics of Tumours of the Digestive System, IARC Press, Lyon, 2000, pp. 157–202.
[23] T. Genda, M. Sakamoto, T. Ichida, H. Asakura, M. Kojiro, S. Narumiya, S. Hirohashi, Cell motility mediated by rho and Rho-associated protein kinase plays a critical role in intrahepatic metastasis of human hepatocellular carcinoma, Hepatology 30 (1999) 1027–1036.
[24] D.F. Daggett, C.A. Boyd, P. Gautier, R.J. Bryson-Richardson, C. Thisse, B. Thisse, S.L. Amacher, P.D. Currie, Developmentally restricted actin-regulatory molecules control morphogenetic cell movements in the zebrafish gastrula, Curr. Biol. 14 (2004) 1632–1638.
[25] D.F. Daggett, C.R. Domingo, P.D. Currie, S.L. Amacher, Control of morphogenetic cell movements in the early zebrafish myotome, Dev. Biol. 309 (2007) 169–179.
[26] B. Baum, W. Li, N. Perrimon, A cyclase-associated protein regulates actin and cell polarity during *Drosophila* oogenesis and in yeast, Curr. Biol. 10 (2000) 964–973.
[27] A.A. Noegel, R. Blau-Wasser, H. Sultana, R. Muller, L. Israel, M. Schleicher, H. Patel, C.J. Weijer, The cyclase-associated protein CAP as regulator of cell polarity and cAMP signaling in *Dictyostelium*, Mol. Biol. Cell 15 (2004) 934–945.
[28] V. Peche, S. Shekar, M. Leichter, H. Korte, R. Schroder, M. Schleicher, T.A. Holak, C.S. Clemen, Y.B. Ramanath, G. Pfitzer, I. Karakesisoglou, A.A. Noegel, CAP2, cyclase-associated protein 2, is a dual compartment protein, Cell. Mol. Life Sci. 64 (2007) 2702–2715.
[29] M. Wolanski, F. Khosrowshahian, L. Jerant, I.S. Jap, J. Brockman, M.J. Crawford, Expression of CAP2 during early *Xenopus* embryogenesis, Int. J. Dev. Biol. 53 (2009) 1063–1067.
[30] S. Sumanas, H.J. Kim, S. Hermanson, S.C. Ekker, Zebrafish frizzled-2 morphant displays defects in body axis elongation, Genesis 30 (2001) 114–118.
[31] D.J. Mawdsley, H.M. Cooper, B.M. Hogan, S.H. Cody, G.J. Lieschke, J.K. Heath, The Netrin receptor Neogenin is required for neural tube formation and somitogenesis in zebrafish, Dev. Biol. 269 (2004) 302–315.
[32] S.C. Little, M.C. Mullins, Twisted gastrulation promotes BMP signaling in zebrafish dorsal–ventral axial patterning, Development 131 (2004) 5825–5835.
[33] T.P. Loisel, R. Boujemaa, D. Pantaloni, M.F. Carlier, Reconstitution of actin-based motility of *Listeria* and *Shigella* using pure proteins, Nature 401 (1999) 613–616.
[34] T.D. Pollard, L. Blanchoin, R.D. Mullins, Molecular mechanisms controlling actin filament dynamics in nonmuscle cells, Annu. Rev. Biophys. Biomol. Struct. 29 (2000) 545–576.
[35] A. Hubberstey, G. Yu, R. Loewith, C. Lakusta, D. Young, Mammalian CAP interacts with CAP, CAP2, and actin, J. Cell. Biochem. 61 (1996) 459–466.
[36] K. Yamazaki, M. Takamura, Y. Masugi, T. Mori, W. Du, T. Hibi, N. Hiraoka, T. Ohta, M. Ohki, S. Hirohashi, M. Sakamoto, Adenylate cyclase-associated protein 1 overexpressed in pancreatic cancers is involved in cancer cell motility, Lab. Invest. 89 (2009) 425–432.
[37] J. Chu, K.C. Sadler, New school in liver development: lessons from zebrafish, Hepatology 50 (2009) 1656–1663.
[38] S.H. Lam, Y.L. Wu, V.B. Vega, L.D. Miller, J. Spitsbergen, Y. Tong, H. Zhan, K.R. Govindarajan, S. Lee, S. Mathavan, K.R. Murthy, D.R. Buhler, E.T. Liu, Z. Gong, Conservation of gene expression signatures between zebrafish and human liver tumors and tumor progression, Nat. Biotechnol. 24 (2006) 73–75.

Antiviral Therapy 2012; 17:35–43 (doi: 10.3851/IMP1923)

Original article

Age and total ribavirin dose are independent predictors of relapse after interferon therapy in chronic hepatitis C revealed by data mining analysis

*Masayuki Kurosaki[1], Naoki Hiramatsu[2], Minoru Sakamoto[3], Yoshiyuki Suzuki[4], Manabu Iwasaki[5], Akihiro Tamori[6], Kentaro Matsuura[7], Sei Kakinuma[8], Fuminaka Sugauchi[9], Naoya Sakamoto[8], Mina Nakagawa[8], Hiroshi Yatsuhashi[10], Namiki Izumi[1]**

[1]Division of Gastroenterology and Hepatology, Musashino Red Cross Hospital, Tokyo, Japan
[2]Department of Gastroenterology and Hepatology, Osaka University Graduate School of Medicine, Osaka, Japan
[3]First Department of Internal Medicine, University of Yamanashi, Yamanashi, Japan
[4]Department of Hepatology, Toranomon Hospital, Tokyo, Japan
[5]Department of Computer and Information Science, Seikei University, Tokyo, Japan
[6]Department of Hepatology, Osaka City University Medical School, Osaka, Japan
[7]Department of Gastroenterology and Metabolism, Nagoya City University Graduate School of Medical Sciences, Nagoya, Japan
[8]Department of Gastroenterology and Hepatology, Tokyo Medical and Dental University, Tokyo, Japan
[9]Department of Gastroenterology, Nagoya Koseiin Medical Welfare Center, Nagoya, Japan
[10]Clinical Research Center, National Nagasaki Medical Center, Nagasaki, Japan

*Corresponding author e-mail: nizumi@musashino.jrc.or.jp

Background: This study aimed to define factors associated with relapse among responders to pegylated interferon (PEG-IFN) plus ribavirin (RBV) therapy in chronic hepatitis C.

Methods: A cohort of genotype 1b chronic hepatitis C patients treated with PEG-IFN plus RBV and who had an undetectable HCV RNA by week 12 (n=951) were randomly assigned to model derivation (n=636) or internal validation (n=315) groups. An independent cohort (n=598) were used for an external validation. A decision tree model for relapse was explored using data mining analysis.

Results: The data mining analysis defined five subgroups of patients with variable rates of relapse ranging from 13% to 52%. The reproducibility of the model was confirmed by internal and external validations (r^2=0.79 and 0.83, respectively). Patients with undetectable HCV RNA at week 4 had the lowest risk of relapse (13%), followed by patients <60 years with undetectable HCV RNA at week 5–12 who received ≥3.0 g/kg of body weight of RBV (16%). Older patients with a total RBV dose <3.0 g/kg had the highest risk of relapse (52%). Higher RBV dose beyond 3.0 g/kg was associated with further decrease of relapse rate among patients <60 years (up to 11%) but not among older patients whose relapse rate remained stable around 30%.

Conclusions: Data mining analysis revealed that time to HCV RNA negativity, age and total RBV dose was associated with relapse. To prevent relapse, ≥3.0 g/kg of RBV should be administered. Higher dose of RBV may be beneficial in patients <60 years.

Introduction

The currently recommended therapy for chronic hepatitis C is a combination of pegylated interferon (PEG-IFN) plus ribavirin (RBV) [1]. This therapy is effective in 50% of patients with HCV genotype 1b [2,3]. The most reliable predictor of sustained virological response (SVR) is the response during early weeks of therapy. A satisfactory response to therapy in the early weeks is associated with a high rate of SVR [4–8]. A basic concept of response-guided therapy is to modify the duration of therapy according to the time to HCV RNA negativity. Extended therapy may be given to patients with delayed virological response [9–13]. Modification of duration of therapy or drug dose may also be necessary in patients with early virological

©2012 International Medical Press 1359-6535 (print) 2040-2058 (online)

response (EVR), because approximately 20% of these patients experience relapse after the completion of 48 weeks of therapy. Recent reports have revealed that single nucleotide polymorphisms located near the *IL28B* gene are strongly associated with SVR or a null response to PEG-IFN plus RBV therapy [14–16]. However, single nucleotide polymorphisms located near the *IL28B* gene are not associated with relapse after EVR [17]. Identification of risk factors for relapse among patients with virological response may lead to more individualized therapy and improved SVR rate.

Decision tree analysis, a core component of data mining analysis, is a method that explores data to develop predictive models [18]. This method has been originally used in business and recently in medical fields [19–25]. Decision tree analysis was successfully used to build a predictive model of EVR [26] and SVR to PEG-IFN plus RBV combination therapy in chronic hepatitis C [17,27,28]. The results of the analysis are presented as a tree structure, which is easy to understand and use in clinical practice. Patients can be allocated into subgroups by simply following the flowchart form of the decision tree [29].

In the present study, we used decision tree analysis to identify predictors of relapse among patients who achieved EVR to PEG-IFN plus RBV therapy, and to define a more individualized therapeutic strategy beyond response-guided therapy.

Table 1. Background of study population

Characteristic	Value
Age, years	54.9 (10.8)
Gender	–
Male, *n* (%)	557 (59)
Female, *n* (%)	394 (41)
Body mass index, kg/m^2	23.2 (3.3)
Albumin, g/dl	4.1 (1.8)
Creatinine, mg/dl	0.7 (0.2)
AST, IU/l	60.6 (46.2)
ALT, IU/l	80.7 (77.2)
GGT, IU/l	52.0 (60.0)
White blood cell count, cells/μl	4,993 (1,363)
Haemoglobin, g/dl	15.9 (52.6)
Platelets, 10^9/l	174.4 (6.1)
HCV RNA, KIU/ml	1,655 (1,455)
Fibrosis stage	–
F1-2, *n* (%)	626 (66)
F3-4, *n* (%)	98 (10)
NA, *n* (%)	227 (24)
Time to HCV RNA negativity 4/8/12 weeks	–
4 Weeks, *n* (%)	233 (24)
8 Weeks, *n* (%)	386 (41)
12 Weeks, *n* (%)	332 (35)
Treatment duration, weeks	42 (13)
Total RBV dose, g/kg body weight	3.1 (1.3)
Total PEG-IFN dose, μg/kg body weight	62.5 (38.6)
Outcome	–
Relapse, *n* (%)	238 (25)
SVR, *n* (%)	713 (75)

Total *n*=951. Data are expressed as mean (SD) unless otherwise indicated. ALT, alanine aminotransferase; AST, aspartate aminotransferase; GGT, γ-glutamyltransferase; NA, not available; PEG-IFN, pegylated interferon; RBV, ribavirin; SVR: sustained virological response.

Methods

Patients

This is a multicentre retrospective cohort study involving Musashino Red Cross Hospital, Toranomon Hospital, Tokyo Medical and Dental University, Osaka University, Nagoya City University, Yamanashi University, Osaka City University, and their related hospitals. The inclusion criteria were chronic hepatitis C patients treated with PEG-IFN-α2b plus RBV, genotype 1b, pretreatment HCV RNA titre >100 KIU/ml as confirmed by quantitative PCR; Cobas Amplicor HCV Monitor version 2.0; Roche Diagnostic Systems, Pleasanton, CA, USA), an undetectable HCV RNA level within week 12 after the start of therapy, no coinfection with HBV or HIV, and no other causes of liver disease. Patients were treated with PEG-IFN-α2b (1.5 μg/kg) subcutaneously every week plus a daily weight-adjusted RBV dose (600 mg for patients weighing <60 kg, 800 mg for patients weighing 60–80 kg and 1,000 mg for patients weighing >80 kg). Dose reduction or discontinuation of PEG-IFN and RBV was considered based on the recommendations of the package inserts and the discretion of physicians at each university and hospital. The standard duration of therapy was set at 48 weeks, but extension of duration was allowed and implemented at the discretion of each physician. The duration of therapy was extended beyond 48 weeks in 118 patients (mean duration was 56.3 weeks, ranging from 49 to 72 weeks). Although the exact reason for the prolonged treatment in each case was not available, one reason may be that each physician tried to achieve high adherence of RBV by extending the duration of therapy. Another reason may be the late time point of HCV RNA negativity even within early virological response. Among 118 patients, time to HCV RNA negativity was between 9 to 12 weeks in 56% of patients.

A total of 951 patients fulfilled the study criteria. The baseline characteristics and representative laboratory test results are listed in Table 1. For analysis, patients were randomly assigned to either the model derivation (636 patients) or internal validation (315 patients) groups. There were no significant differences in the clinical backgrounds between these two groups. For external validation of the model, we collaborated with another multicentre study group consisting of 29 medical centres and hospitals belonging to the National

©2012 International Medical Press

Hospital Organization (Japan). A dataset collected from 598 patients who were treated with PEG-IFN-α2b plus RBV and had undetectable HCV RNA within week 12 were used for external validation. Informed consent was obtained from each patient. The study protocol conformed to the ethical guidelines of the Declaration of Helsinki and was approved by the institutional review committees of all concerned hospitals.

Laboratory tests

Haematological tests, blood chemistry and HCV RNA titre were analysed before therapy and at least once every month during therapy. Rapid virological response (RVR) was defined as an undetectable HCV RNA level at week 4, and complete early virological response (cEVR) was defined as an undetectable HCV RNA level at week 5 through week 12 after the start of therapy. SVR was defined as an undetectable HCV RNA level 24 weeks after the completion of therapy. Detection of HCV RNA level was based on qualitative PCR with a lower detection limit of 50 IU/ml (Amplicor; Roche Diagnostic Systems). A database of pretreatment variables included haematological tests (haemoglobin level, white blood cell count and platelet count), blood chemistry tests (serum levels of creatinine, albumin, aspartate aminotransferase, alanine aminotransferase, γ-glutamyltransferase, total cholesterol, triglycerides and HCV RNA titre), stage of histological fibrosis and patient characteristics (age, sex and body mass index). Post-treatment variables included time to HCV RNA negativity, calculated total RBV dose (g/kg of body weight), and calculated total PEG-IFN dose (μg/kg of body weight).

Statistical analysis

The Student's *t*-test was used for the univariable comparison of quantitative variables and Fisher's exact test was used for the comparison of qualitative variables. Logistic regression models with backward selection procedures were used for multivariable analysis of factors associated with relapse. IBM SPSS software version 18.0 (SPSS Inc., Chicago, IL, USA) was used for analysis. For the decision tree analysis [30], the data mining software IBM SPSS Modeler 14 (SPSS Inc.) was used, as reported previously [17,26–28]. The decision tree analysis, the core component of the data mining, belongs to a family of non-parametric regression methods based on binary recursive partitioning of data. In this analysis, the software automatically explored the database to determine optimal split variables to build a decision tree structure. A statistical search algorithm evaluate the model derivation group to determine the optimum variables and cutoff values and to yield the most significant division of patients into two subgroups that were as homogeneous as possible for the probability of relapse. Once patients were divided into 2 subgroups, the analysis was automatically repeated on each subgroup in the same way until either no additional significant variable was detected or the number of patients was <20. Finally all patients were classified into particular subgroups that are homogeneous with respect to the probabilities of relapse.

Results

The decision tree model for the prediction of relapse

The overall rate of relapse was 26% in the model derivation group. The decision tree analysis selected three variables that are associated with relapse: time to HCV RNA negativity, age and total RBV dose (Figure 1). Time to HCV RNA negativity was selected as the best predictor of relapse. The rate of relapse was 13% for patients with RVR compared to 30% for patients with cEVR. Among patients with cEVR, age was selected as the variable of second split. Patients <60 years had a lower probability of relapse (22%) compared with those ≥60 years (41%). The total RBV dose was selected as the third variable of split with an optimal cutoff of 3.0 g/kg of body weight. The rate of relapse was lower in patients who received ≥3.0 g/kg of body weight of RBV compared to patients who received <3.0 g/kg of body weight (among patients <60 years rates were 16% versus 32% and among patients ≥60 years rates were 26% versus 52%, respectively).

According to this decision tree, the patients were divided into five groups with different rates of relapse ranging from 13% to 52%. Patients with RVR had the lowest risk of relapse. Among patients with cEVR, patients <60 years who received ≥3.0 g/kg of body weight of RBV also had a low risk of relapse (16%). By contrast, patients who received <3.0 g/kg of body weight of RBV had higher than the average risk of relapse, especially in patients ≥60 years (52%).

Validation of the decision tree model

The decision tree model was validated using an internal validation group that was not included in the model derivation. The rates of relapse for each subgroup of patients were correlated closely between the model derivation and the internal validation group (r^2=0.79; Figure 2A). When validated using an external validation group, the rates of relapse for each subgroup of patients were again correlated closely between the model derivation and the external validation group. (r^2=0.83; Figure 2B).

Multivariable logistic regression analysis for factors associated with relapse

Univariable and multivariable analysis was performed using the combined population of model derivation and internal validation group. Univariable analysis found

that age, sex, serum levels of creatinine, haemoglobin, platelet count, HCV RNA titre, time to HCV RNA negativity, total PEG-IFN dose and total RBV dose were associated with relapse. Duration of therapy was not associated with reduction in relapse rate. Multivariable analysis including these factors showed that age, total RBV dose, serum level of creatinine, and time to HCV RNA negativity were independent predictors of relapse (Table 2). Creatinine was not selected as a splitting variable in data mining analysis probably due to the limitation to stop the analysis when the number of patients was <20. Using the combined population of model derivation and internal validation group, patients in each subgroup of decision tree model were further stratified by creatinine levels and the effect of creatinine level on relapse was analysed. Among patients with RVR, the rate of relapse did not differ between patients with creatinine levels of <0.7 g/dl and ≥0.7 g/dl and were 12% and 12%, respectively. Among patients with cEVR, the rate of relapse was higher in patients with creatinine levels of <0.7 g/dl compared to those with creatinine levels of ≥0.7 g/dl and were 39% versus 23%, respectively, for patients <60 years who received <3.0 g/kg of body weight of RBV, 19% versus 14% for patients <60 years who received ≥3.0 g/kg of body weight of RBV, 58% versus 41% for patients ≥60 years who received <3.0 g/kg of body weight of RBV, and 42% versus 26% for patients ≥60 years who received ≥3.0 g/kg of body weight of RBV.

Effect of age and total RBV dose on relapse among patients with cEVR

The effect of total RBV dose on relapse was analysed among patients with cEVR in a combined group of

Figure 1. The decision-tree model of relapse among patients with rapid virological response or complete early virological response

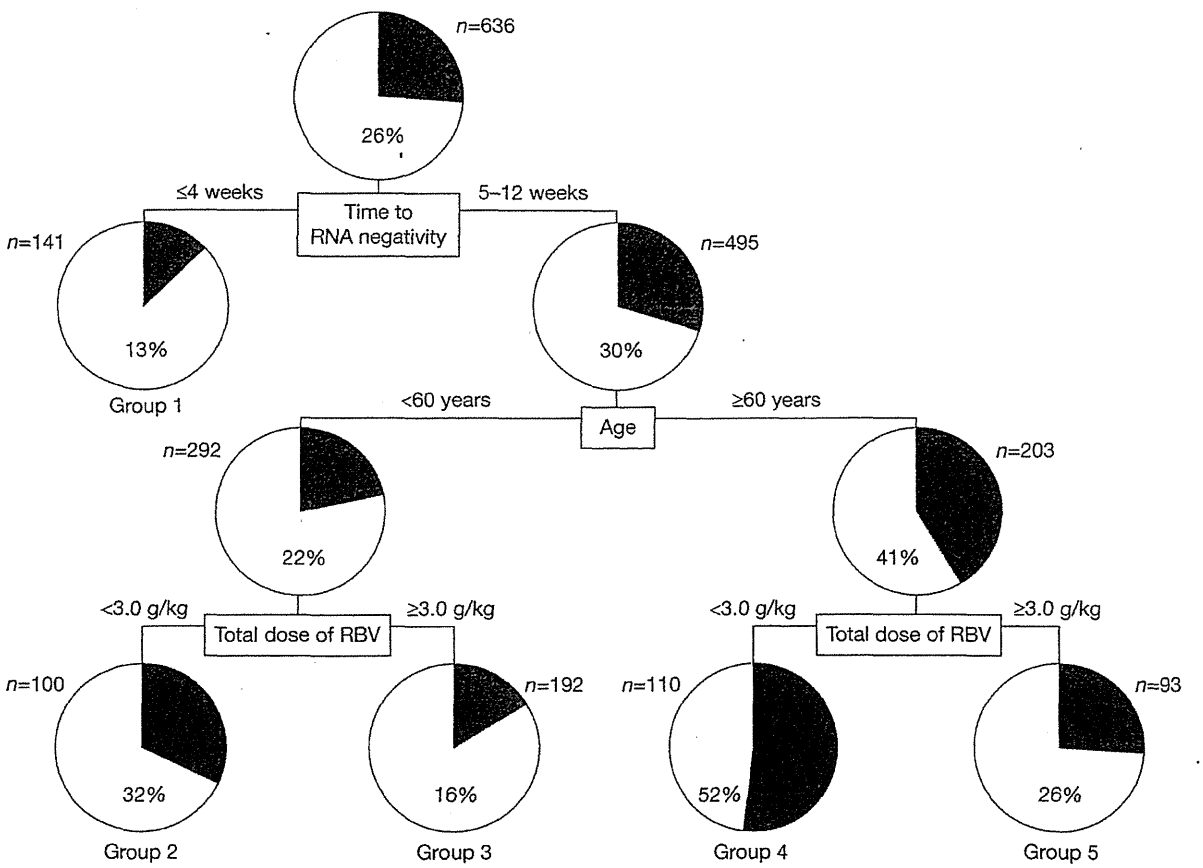

Boxes indicate the factors used for splitting and the cutoff values for the split. Pie charts indicate the rate of relapse for each group of patients after splitting. Terminal groups of patients discriminated by the analysis are numbered from 1 to 5. The rate of relapse was higher than average (>26%) in subgroups 2 and 4, where total ribavirin (RBV) dose was <3 g/kg of body weight.

©2012 International Medical Press

model derivation and internal validation (n=718). The relapse rate decreased with an increase in RBV dose (Figure 3A). When patients were stratified into two groups according to age, the relapse rate decreased with an increase in RBV dose in patients <60 years. The relapse rate was lowest (11%) in patients <60 years who received ≥4.0 g/kg of body weight of RBV. By contrast, among patients ≥60 years, the relapse rate decreased with an increase in RBV dose up to 3.0 g/kg of body weight, but remained relatively stable despite a further increase in the RBV dose beyond 3.0 g/kg of body weight. The rate of relapse was 31% to 33% in patients who received ≥3.0 g/kg of body weight. Patients ≥60 years had higher relapse rate compared with patients <60 years after stratification by RBV dose (P=0.044 for RBV <2.5 g/kg, P=0.009 for RBV 2.5–2.9 g/kg, P=0.150 for RBV 3.0–3.4 g/kg, P=0.036 for RBV 3.5–3.9 g/kg and P=0.006 for RBV ≥4.0 g/kg).

To exclude the effect of the duration of therapy, patients who received 42–54 weeks of therapy were selected (n=544). Again, the relapse rate decreased with an increase in RBV dose in patients <60 years but remained stable despite a further increase in the RBV dose beyond 3.0 g/kg of body weight in patients ≥60 years (Figure 3B); in addition, patients ≥60 years had a higher relapse rate compared with younger patients after stratification by

Figure 2. Internal and external validation of the decision-tree model: subgroup-stratified comparison of the rate of relapse between the model derivation and validation groups

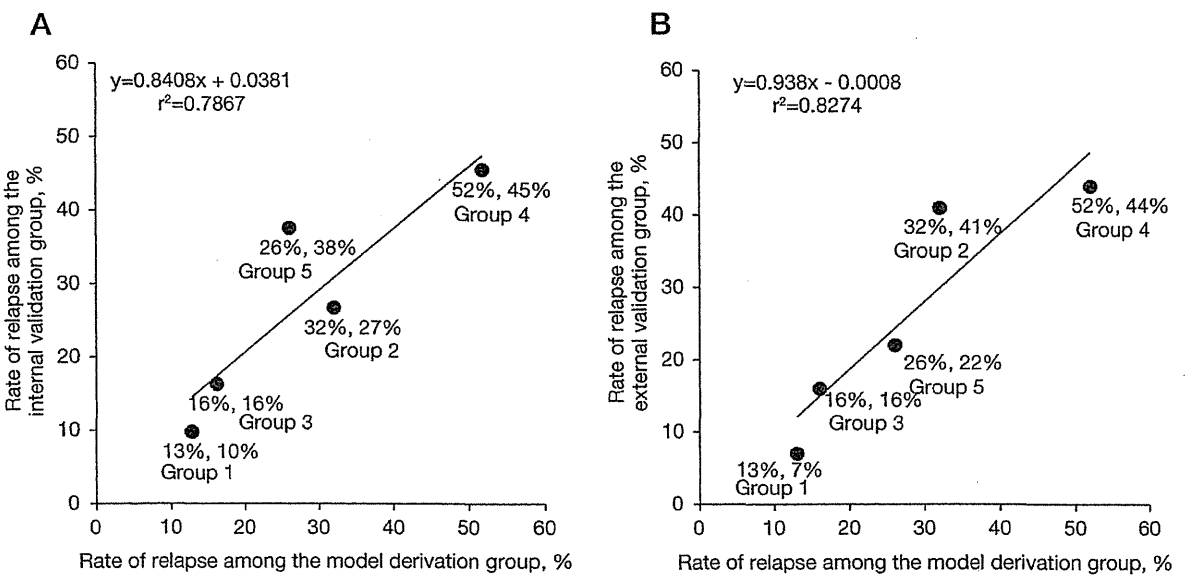

Each patient in the internal and external validation population was allocated to groups 1 to 5 following the flowchart of the decision tree. The rates of relapse were then calculated for each group and a graph was plotted. The rate of relapse in the (A) internal and (B) external validation groups are shown. The rates of relapse are shown as percentages below data points: the value on the left is from the model derivation group and on the right is from the validation group. The rates of relapse in each group of patients correlated closely between the model derivation group and the validation group (correlation coefficient: r^2=0.79 and 0.83, respectively).

Table 2. Multivariable analysis of factors associated with relapse among patients with RVR/cEVR

Factor	OR	95% CI	P-value
No-RVR	4.07	2.57–6.43	<0.0001
Total RBV dose <3.0 g/kg body weight	2.19	1.58 –3.03	<0.0001
Creatinine <0.7 g/dl	1.67	1.22–2.29	0.001
Age ≥60 years	2.37	1.73–3.24	<0.0001

cEVR, complete early virological response (HCV-RNA-positive at week 4, but negative at week 12); RBV, ribavirin; RVR, rapid virological response (HCV-RNA-negative at week 4).

RBV dose (P=0.283 for RBV <2.5 g/kg, P=0.017 for RBV 2.5–2.9 g/kg, P=0.127 for RBV 3.0–3.4 g/kg, P=0.011 for RBV 3.5–3.9 g/kg and P=0.009 for RBV ≥4.0 g/kg).

Total dose of RBV was associated with relapse independently of PEG-IFN dose. The cutoff value of 58 zμg/kg of PEG-IFN was selected, which corresponds to the 80% of 1.5 μg/kg dose for 48 weeks. In patients who received <58 μg/kg of body weight of PEG-IFN, the rate of relapse for patients who received ≥3.0 g/kg or <3.0 g/kg of body weight of RBV was 24% and 42%, respectively. In patients who received ≥58 μg/kg of body weight of PEG-IFN, the rate of relapse for patients who received ≥3.0 g/kg or <3.0 g/kg of body weight of RBV was 21% and 38%, respectively.

The data mining analysis procedure did not select further split variables among RVR patients. However,

Figure 3. Correlation between the rate of relapse and total RBV dose among patients with cEVR after stratification by age

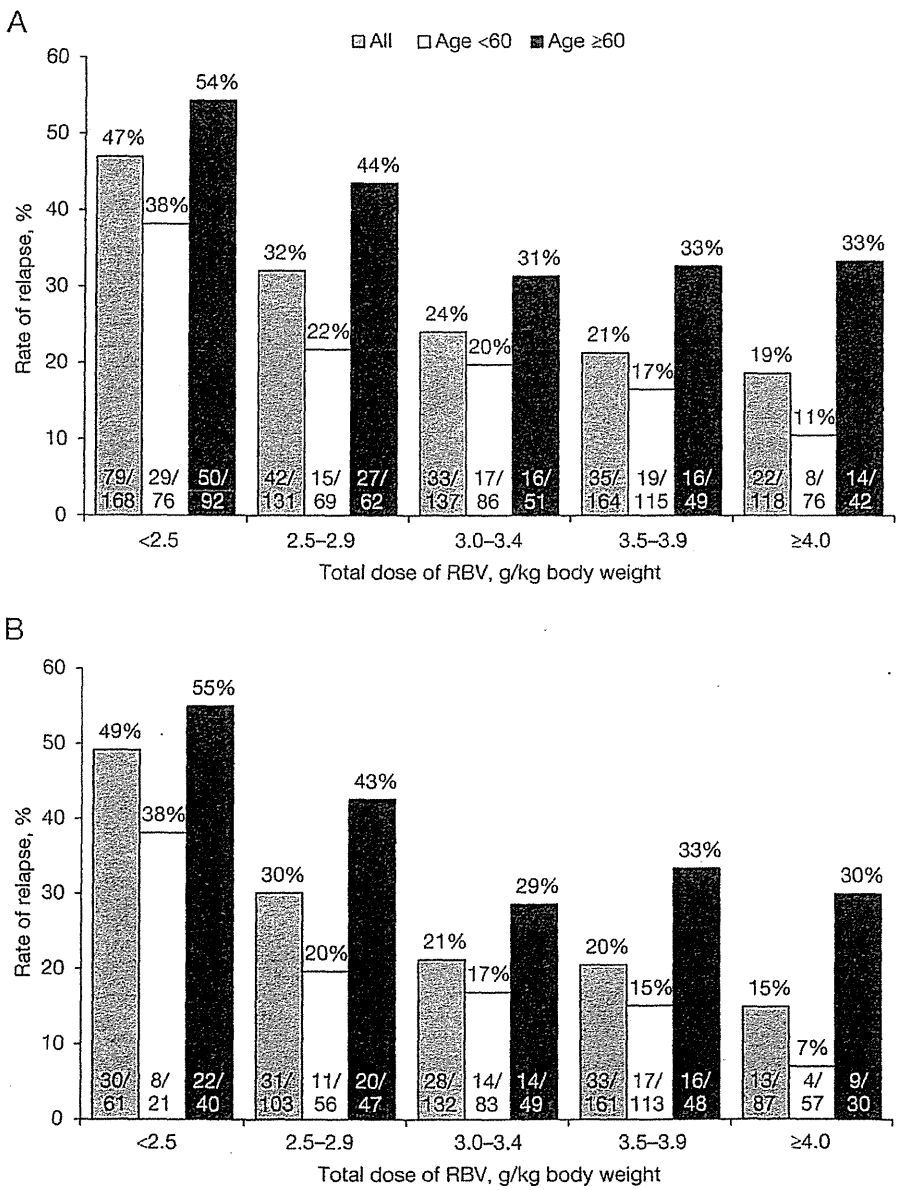

Association between the total ribavirin (RBV) dose and the rate of relapse among patients with complete early virological response (cEVR) is shown. (A) Higher dose of RBV was associated with reduced rate of relapse. (B) These associations were also confirmed in selected patients who received 42–54 weeks of therapy.

©2012 International Medical Press

when analysed separately, the rate of relapse was also associated with age and total RBV dose among patients with RVR. The rate of relapse for patients who received ≥3.0 g/kg or <3.0 g/kg of body weight of RBV was 5% and 14%, respectively. The rate of relapse for patients <60 and ≥60 years was 9% and 18%, respectively. Collectively, the rate of relapse for patients <60 years who received ≥3.0 g/kg or <3.0 g/kg of body weight of RBV was 2% and 11%, respectively, whereas the rate of relapse for patients ≥60 years who received ≥3.0 g/kg or <3.0 g/kg of body weight of RBV was 12% and 20%, respectively.

Discussion

The result of the present study shows that older age and insufficient dose of RBV are significant and independent risk factors for relapse among patients with cEVR to PEG-IFN plus RBV. Older patients (≥60 years) who received a total RBV dose <3.0 g/kg of body weight had the highest risk of relapse (52%), whereas younger patients who received a total RBV dose ≥3.0 g/kg of body weight had the lowest risk of relapse (16%). The rate of relapse decreased depending on the total RBV dose in younger patients, but remained stable in older patients despite a further increase in the RBV dose beyond 3.0 g/kg of body weight. These findings imply that the target dose of total RBV can be set at 3.0 g/kg of body weight in patients who achieved cEVR, and further increase in RBV dose up to 4.0 g/kg of body weight or greater may be recommended in patients <60 years.

The associations between the drug adherence and virological response had been reported with inconsistent results. In an earlier study, patients who received >80% of the planned dose of PEG-IFN plus RBV for >80% of the planned duration of therapy had a higher rate of SVR compared to those who received a lesser dose (51% versus 34%) [31]. Consistent results were obtained in a study reporting that patients who received >80% of the planned dose of PEG-IFN and RBV within the first 12 weeks of therapy had a higher rate of EVR compared with those who received a lesser dose of both drugs (80% versus 33%) [4]. By contrast, a large-scale multicentre study showed that reducing the PEG-IFN dose during the first 20 weeks reduced SVR; however, reducing RBV did not affect SVR as long as RBV was not prematurely discontinued [32]. The reason for these inconsistencies is unclear. One reason may be the differences in the backgrounds of patients enrolled in the study, and hence the last study was limited to patients with advanced fibrosis and prior non-responders to PEG-IFN therapy. Because the probability of SVR is affected by virological response and relapse after response, the effect of drug dosing should be analysed separately with respect to these two factors.

In the present study, we focused on factors predictive of relapse after early virological response. According to the decision tree model, relapse was less likely in patients with RVR compared with cEVR. Among patients with cEVR, older patients (≥60 years) had a higher risk of relapse compared to younger patients (41% versus 22%). In addition, our results emphasized the effect of RBV dose for the prevention of relapse. In our study, a total RBV dose of ≥3.0 g/kg of body weight was repeatedly associated with a suppressed rate of relapse in the model derivation and validation groups. The rate of relapse in patients <60 years who received an RBV dose of <3.0 versus ≥3.0 g/kg of body weight in the model derivation, internal validation and external validation groups were 32% versus 16%, 27% versus 16%, and 41% versus 16%, respectively. The rate of relapse in patients ≥60 years who received an RBV dose of <3.0 versus ≥3.0 g/kg of body weight in the model derivation, internal validation and external validation groups were 52% versus 26%, 45% versus 38%, and 44% versus 22%, respectively. It has been reported that the rate of relapse is suppressed in 48 weeks of IFN plus RBV combination therapy compared to IFN monotherapy, indicating that RBV contributes to the increase in SVR by reducing relapse [2,3]. Another study, focused on the associations between the drug dose reduction and relapse in patients with virological response, found that maintaining RBV dose ≥12 mg/kg/day during 48 weeks of treatment, which can be translated into a total dose of 4.0 g/kg of body weight, suppressed relapse [33]. Results of the present study are in accordance with this report.

The importance of drug dosing on reduction in relapse is also supported by the findings that extending therapy from 48 to 72 weeks in patients with delayed virological response improved SVR rates by reducing relapse [9–13]. Apart from these clinical studies, in the real world of clinical practice, duration of therapy is extended – even in patients with cEVR – at the physician's discretion. The relationship between duration of therapy or RBV dose, and relapse among patients with cEVR and treated with various lengths of therapy has not been examined. In the combined group of our study, extending the duration of therapy was not associated with a reduction in relapse rate. Rather, the rate of relapse decreased depending on the total RBV dose. These findings suggest that acquiring a sufficient total RBV dose, either within 48 weeks or by extending the duration of therapy, is essential to prevent relapse among patients with cEVR. The limitation of the present study was that the mean duration of therapy was only 56.3 weeks in patients whose duration of therapy was extended beyond 48 weeks. It is probable that extended duration of therapy was not long enough for the prevention of relapse. Further studies with

longer durations of therapy are necessary to confirm the effect of extended duration of therapy on reduction of relapse among patients with cEVR.

Previous reports did not consider the effects of age in setting the optimal dose of RBV. In the present study, the relapse rate decreased with an increase in RBV dose from <2.5 to 3.0–3.5 g/kg of body weight, but remained relatively stable despite a further increase in the RBV dose in older patients. Thus, a total RBV dose ≥3.0 g/kg of body weight should be the target dose for patients ≥60 years with cEVR. By contrast, ≥3.0 g/kg of body weight of RBV was associated with lower risk of relapse in patients <60 with cEVR (16% versus 32%), and a further increase in RBV dose led to a more profound reduction in relapse rates, as low as 11% in patients who received ≥4.0 g/kg of body weight. Thus, a total dose of ≥4.0 g/kg of body weight or even greater should be the target dose in patients <60 years.

In the near future, more potent therapies, such as direct antiviral agents [34,35], may become available. These drugs require RBV and PEG-IFN in combination. However, not all patients may be able to tolerate this triple combination therapy due to adverse drug reactions, such as severe anaemia or skin eruption. In particular, it may be difficult to administer a full dose of triple drugs to older patients. Thus, personalizing the PEG-IFN and RBV combination therapy based on this model may be beneficial to patients who were intolerant to triple combination therapy.

In the present study creatinine was an independent predictor of relapse by multivariable logistic regression analysis. However creatinine was not selected as a splitting variable in decision tree, which may be due to the unique property of data mining analysis. In data mining analysis, limitation is imposed to stop the analysis when the number of patients is <20. This limitation is used to avoid dividing patients into too small subgroups which lead to the generation of rules that only apply to the model derivation population and not reproduced when applied to other populations. This phenomenon is called the over-fitting of the model. Due to this limitation, the variables selected in the data mining analysis are not necessarily identical to the variables that are significant by ordinary multivariable analysis. In a separate analysis, lower level of creatinine was associated with higher rate of relapse in each subgroup of patients with cEVR. The reason for this association is not clear, but lower creatinine level may be related to more efficient clearance of RBV leading to lower serum level of RBV. Further research is needed to confirm this speculation.

A potential limitation of the present study is that data mining analysis has an intrinsic risk of showing relationships that fit to the original dataset, but are not reproducible in different groups. Although internal and external validations showed that our model had high reproducibility, we recognized that further validation on a larger external validation cohort, especially in groups other than Japanese, may be necessary to further verify the reliability of our model.

In conclusion, we built a decision tree model for the prediction of relapse among patients with EVR to PEG-IFN plus RBV. The result of the present study shows that older age and insufficient dose of RBV are significant and independent risk factors for relapse. The target dose of total RBV can be set at 3.0 g/kg of body weight in patients who achieved cEVR. A further increase in RBV dose up to 4.0 g/kg of body weight may be warranted in patients <60 years.

Acknowledgements

This study was supported by a Grant-in-Aid from the Ministry of Health, Labor and Welfare, Japan (H20-kanen-006).

Disclosure statement

The authors declare no competing interests.

References

1. Strader DB, Wright T, Thomas DL, Seeff LB. Diagnosis, management, and treatment of hepatitis C. *Hepatology* 2004; 39:1147–1171.
2. Fried MW, Shiffman ML, Reddy KR, *et al.* Peginterferon alfa-2a plus ribavirin for chronic hepatitis C virus infection. *N Engl J Med* 2002; 347:975–982.
3. Manns MP, McHutchison JG, Gordon SC, *et al.* Peginterferon alfa-2b plus ribavirin compared with interferon alfa-2b plus ribavirin for initial treatment of chronic hepatitis C: a randomised trial. *Lancet* 2001; 358:958–965.
4. Davis GL, Wong JB, McHutchison JG, Manns MP, Harvey J, Albrecht J. Early virologic response to treatment with peginterferon alfa-2b plus ribavirin in patients with chronic hepatitis C. *Hepatology* 2003; 38:645–652.
5. Lee SS, Ferenci P. Optimizing outcomes in patients with hepatitis C virus genotype 1 or 4. *Antivir Ther* 2008; 13 Suppl 1:9–16.
6. Namiki I, Nishiguchi S, Hino K, *et al.* Management of hepatitis C: report of the consensus meeting at the 45th annual meeting of the Japan Society of Hepatology (2009). *Hepatol Res* 2010; 40:347–368.
7. Jensen DM, Morgan TR, Marcellin P, *et al.* Early identification of HCV genotype 1 patients responding to 24 weeks peginterferon alpha-2a (40 kd)/ribavirin therapy. *Hepatology* 2006; 43:954–960.
8. Yu ML, Dai CY, Huang JF, *et al.* Rapid virological response and treatment duration for chronic hepatitis C genotype 1 patients: a randomized trial. *Hepatology* 2008; 47:1884–1893.
9. Berg T, von Wagner M, Nasser S, *et al.* Extended treatment duration for hepatitis C virus type 1: comparing 48 versus 72 weeks of peginterferon-alfa-2a plus ribavirin. *Gastroenterology* 2006; 130:1086–1097.

©2012 International Medical Press

10. Sánchez-Tapias JM, Diago M, Escartin P, *et al.* Peginterferon-alfa2a plus ribavirin for 48 versus 72 weeks in patients with detectable hepatitis C virus RNA at week 4 of treatment. *Gastroenterology* 2006; **131**:451–460.
11. Ferenci P, Laferl H, Scherzer TM, *et al.* Peginterferon alfa-2a/ribavirin for 48 or 72 weeks in hepatitis C genotypes 1 and 4 patients with slow virologic response. *Gastroenterology* 2010; **138**:503–512.e1.
12. Buti M, Lurie Y, Zakharova NG, *et al.* Randomized trial of peginterferon alfa-2b and ribavirin for 48 or 72 weeks in patients with hepatitis C virus genotype 1 and slow virologic response. *Hepatology* 2010; **52**:1201–1207.
13. Pearlman BL, Ehleben C, Saifee S. Treatment extension to 72 weeks of peginterferon and ribavirin in hepatitis c genotype 1-infected slow responders. *Hepatology* 2007; **46**:1688–1694.
14. Tanaka Y, Nishida N, Sugiyama M, *et al.* Genome-wide association of IL28B with response to pegylated interferon-alpha and ribavirin therapy for chronic hepatitis C. *Nat Genet* 2009; **41**:1105–1109.
15. Suppiah V, Moldovan M, Ahlenstiel G, *et al.* IL28B is associated with response to chronic hepatitis C interferon-alpha and ribavirin therapy. *Nat Genet* 2009; **41**:1100–1104.
16. Ge D, Fellay J, Thompson AJ, *et al.* Genetic variation in IL28B predicts hepatitis C treatment-induced viral clearance. *Nature* 2009; **461**:399–401.
17. Kurosaki M, Tanaka Y, Nishida N, *et al.* Pre-treatment prediction of response to pegylated-interferon plus ribavirin for chronic hepatitis C using genetic polymorphism in IL28B and viral factors. *J Hepatol* 2011; **54**:439–448.
18. Breiman LJH, Friedman RA, Olshen CJ, Stone CM. *Classification and regression trees*. 1980. Belmont, CA: Wadsworth.
19. Garzotto M, Park Y, Mongoue-Tchokote S, *et al.* Recursive partitioning for risk stratification in men undergoing repeat prostate biopsies. *Cancer* 2005; **104**:1911–1917.
20. Miyaki K, Takei I, Watanabe K, Nakashima H, Omae K. Novel statistical classification model of type 2 diabetes mellitus patients for tailor-made prevention using data mining algorithm. *J Epidemiol* 2002; **12**:243–248.
21. Averbook BJ, Fu P, Rao JS, Mansour EG. A long-term analysis of 1018 patients with melanoma by classic Cox regression and tree-structured survival analysis at a major referral center: Implications on the future of cancer staging. *Surgery* 2002; **132**:589–604.
22. Leiter U, Buettner PG, Eigentler TK, Garbe C. Prognostic factors of thin cutaneous melanoma: an analysis of the central malignant melanoma registry of the German dermatological society. *J Clin Oncol* 2004; **22**:3660–3667.
23. Valera VA, Walter BA, Yokoyama N, *et al.* Prognostic groups in colorectal carcinoma patients based on tumor cell proliferation and classification and regression tree (CART) survival analysis. *Ann Surg Oncol* 2007; **14**:34–40.
24. Zlobec I, Steele R, Nigam N, Compton CC. A predictive model of rectal tumor response to preoperative radiotherapy using classification and regression tree methods. *Clin Cancer Res* 2005; **11**:5440–5443.
25. Baquerizo A, Anselmo D, Shackleton C, *et al.* Phosphorus ans an early predictive factor in patients with acute liver failure. *Transplantation* 2003; **75**:2007–2014.
26. Kurosaki M, Matsunaga K, Hirayama I, *et al.* A predictive model of response to peginterferon ribavirin in chronic hepatitis C using classification and regression tree analysis. *Hepatol Res* 2010; **40**:251–260.
27. Kurosaki M, Sakamoto N, Iwasaki M, *et al.* Pretreatment prediction of response to peginterferon plus ribavirin therapy in genotype 1 chronic hepatitis C using data mining analysis. *J Gastroenterol* 2011; **46**:401–409.
28. Kurosaki M, Sakamoto N, Iwasaki M, *et al.* Sequences in the interferon sensitivity determining region and core region of hepatitis C virus impact pretreatment prediction of response to peg-interferon plus ribavirin: data mining analysis. *J Med Virol* 2011; **83**:445–452.
29. LeBlanc M, Crowley J. A review of tree-based prognostic models. *Cancer Treat Res* 1995; **75**:113–124.
30. Segal MR, Bloch DA. A comparison of estimated proportional hazards models and regression trees. *Stat Med* 1989; **8**:539–550.
31. McHutchison JG, Manns M, Patel K, *et al.* Adherence to combination therapy enhances sustained response in genotype-1-infected patients with chronic hepatitis C. *Gastroenterology* 2002; **123**:1061–1069.
32. Shiffman ML, Ghany MG, Morgan TR, *et al.* Impact of reducing peginterferon alfa-2a and ribavirin dose during retreatment in patients with chronic hepatitis C. *Gastroenterology* 2007; **132**:103–112.
33. Hiramatsu N, Oze T, Yakushijin T, *et al.* Ribavirin dose reduction raises relapse rate dose-dependently in genotype 1 patients with hepatitis C responding to pegylated interferon alpha-2b plus ribavirin. *J Viral Hepat* 2009; **16**:586–594.
34. Hézode C, Forestier N, Dusheiko G, *et al.* Telaprevir and peginterferon with or without ribavirin for chronic HCV infection. *N Engl J Med* 2009; **360**:1839–1850.
35. McHutchison JG, Everson GT, Gordon SC, *et al.* Telaprevir with peginterferon and ribavirin for chronic HCV genotype 1 infection. *N Engl J Med* 2009; **360**:1827–1838.

Accepted 18 April 2011; published online 21 October 2011